Supporting Information

Table S1. Comparison of reported flexible blade-coated perovskite solar cells with this work.

Device Architecture	No. of Bladed Layers	Solvent System	PCE (%)	Ref
PET/ITO/PTAA/PFN/ MAPI/C60/BCP/Ag	1	DMF	14.58	(Martin et al., 2020)
PET/ITO/PTAA/$Cs_{0.17}FA_{0.85}Pb(I_{0.9}Br_{0.1})_3$/C60/BCP/Ag	2	DMF: NMP	13.02	(Castriotta et al., 2021)
PET/ITO/NiOx:PDA/MAPI/PCBM/BCP/Ag	2	DMF: DMSO	17.3	(Huang et al., 2020)
PET/ITO/SnO2/$Cs_{0.1}FA_{0.9}Pb(I_{0.9}Br_{0.1})_3$/PTAA/Au	2	DMSO/ IPA	14.08	**This Work**
PET/ITO/SnO2/$Cs_{0.1}FA_{0.9}Pb(I_{0.9}Br_{0.1})_3$/PTAA/Au	3	DMSO/ IPA	13.93	**This Work**

Table S2. Summary of J-V Results Obtained from 160 small cells in three different conditions.

Type		V_{OC} (V)	J_{SC} ($mA.cm^{-2}$)	FF (%)	PCE (%)
Incomplete Drying	Best	0.82	18.63	63.9	9.78
	Average	0.72 ± 0.15	12.30 ± 3.66	48.9 ± 16.29	4.69 ± 2.6
Incomplete Drying + LP	Best	1.03	17.95	68.4	12.70
	Average	0.82 ± 0.14	15.30 ± 1.57	55.4 ± 10.5	7.12 ± 2.0
Optimized Drying + LP	Best	1.03	19.18	71.4	14.08
	Average	1.01 ± 0.03	16.9 ± 1.2	65.0 ± 5.0	11.2 ± 1.12

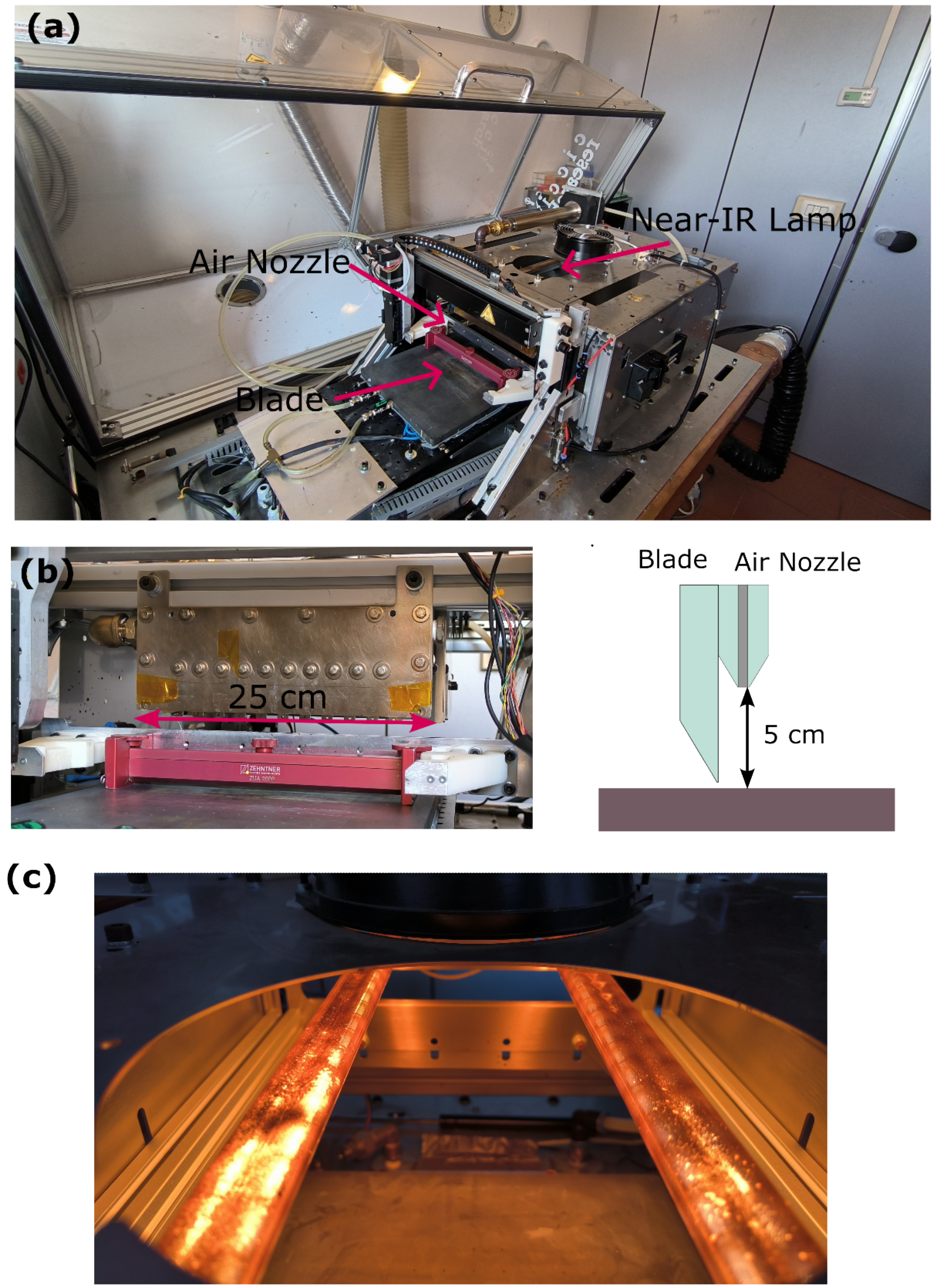

Figure S1- (a) The blade coating machine (Charon by Cicci Research). (b) The blade and air nozzle. (c) The IR drying system using Helios Quartz IR Lamps.

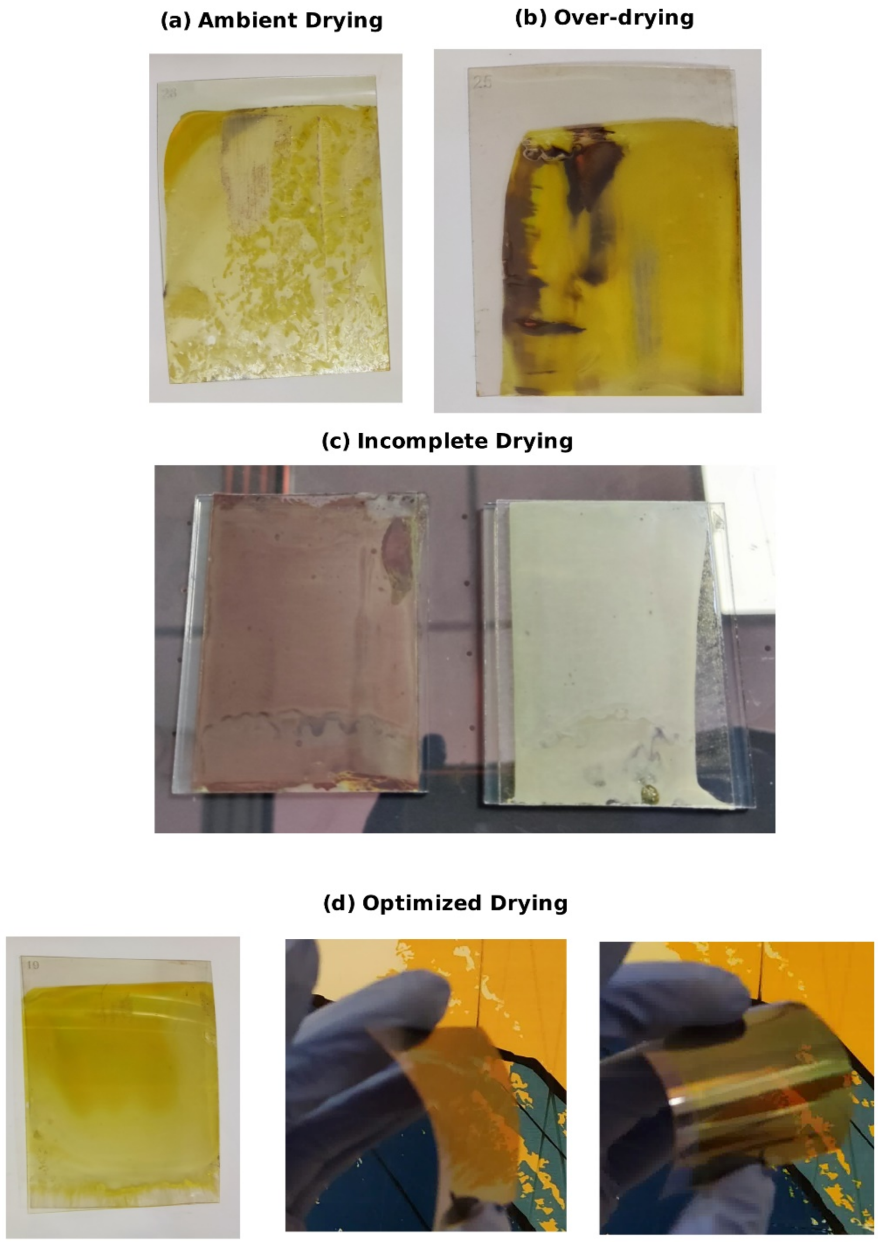

Figure S2. Photographs of PbI_2-$(FAI)_{0.3}$-$(CsI)_{0.15}$ films blade coated in Ambient dried (a) and Over-dried (b) conditions. (c-d) Photographs of both PbI_2-$(FAI)_{0.3}$-$(CsI)_{0.15}$ films and converted perovskite films when the first step is incompletely dried and optimized dried while blading respectively.

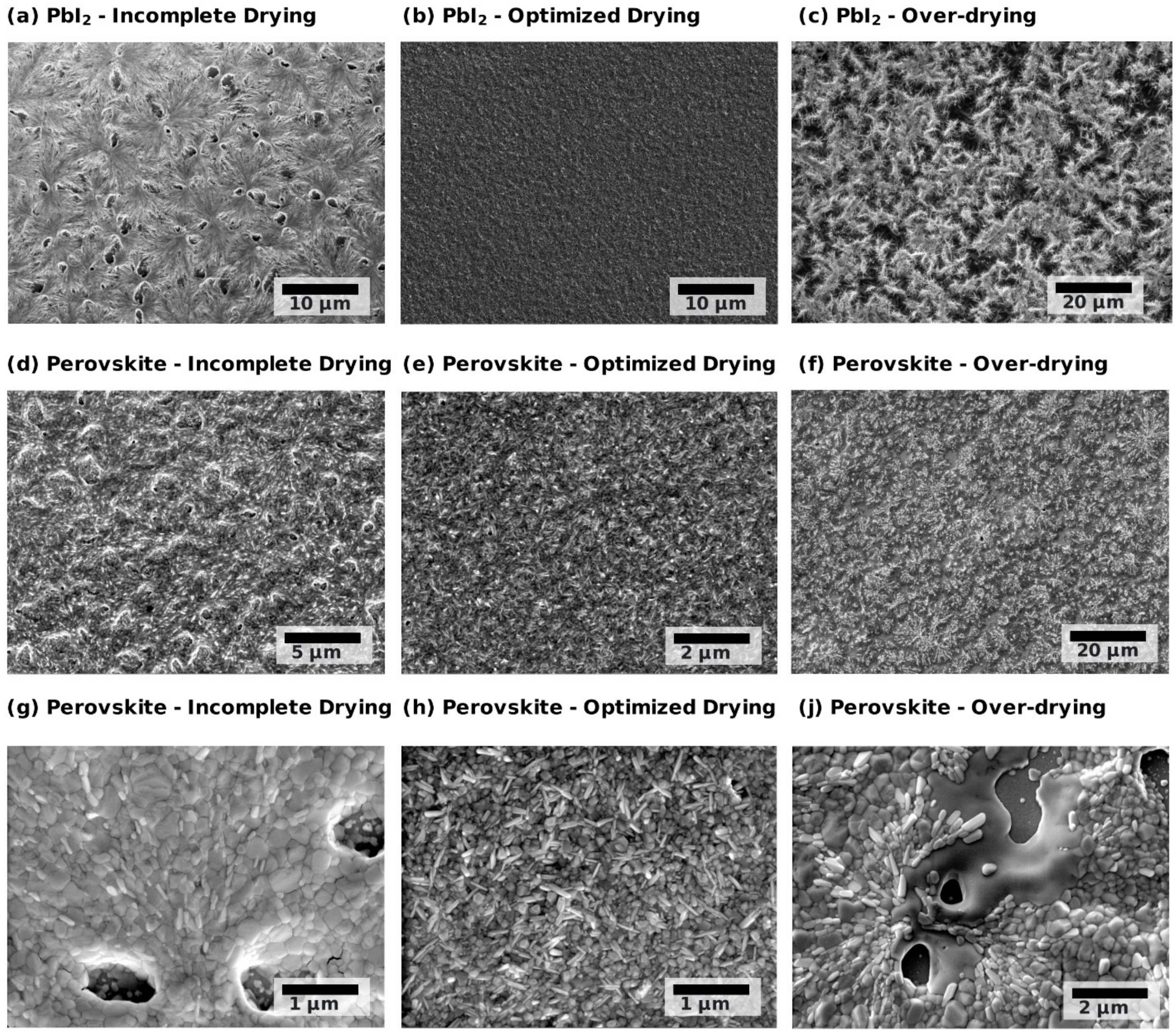

Figure S3. SEM images of blade-coated PbI_2-$(FAI)_{0.3}$-$(CsI)_{0.15}$ (a-c) and their corresponding double cation perovskite layer (d-j) deposited with three different drying conditions of incomplete drying, optimized drying, and over-drying.

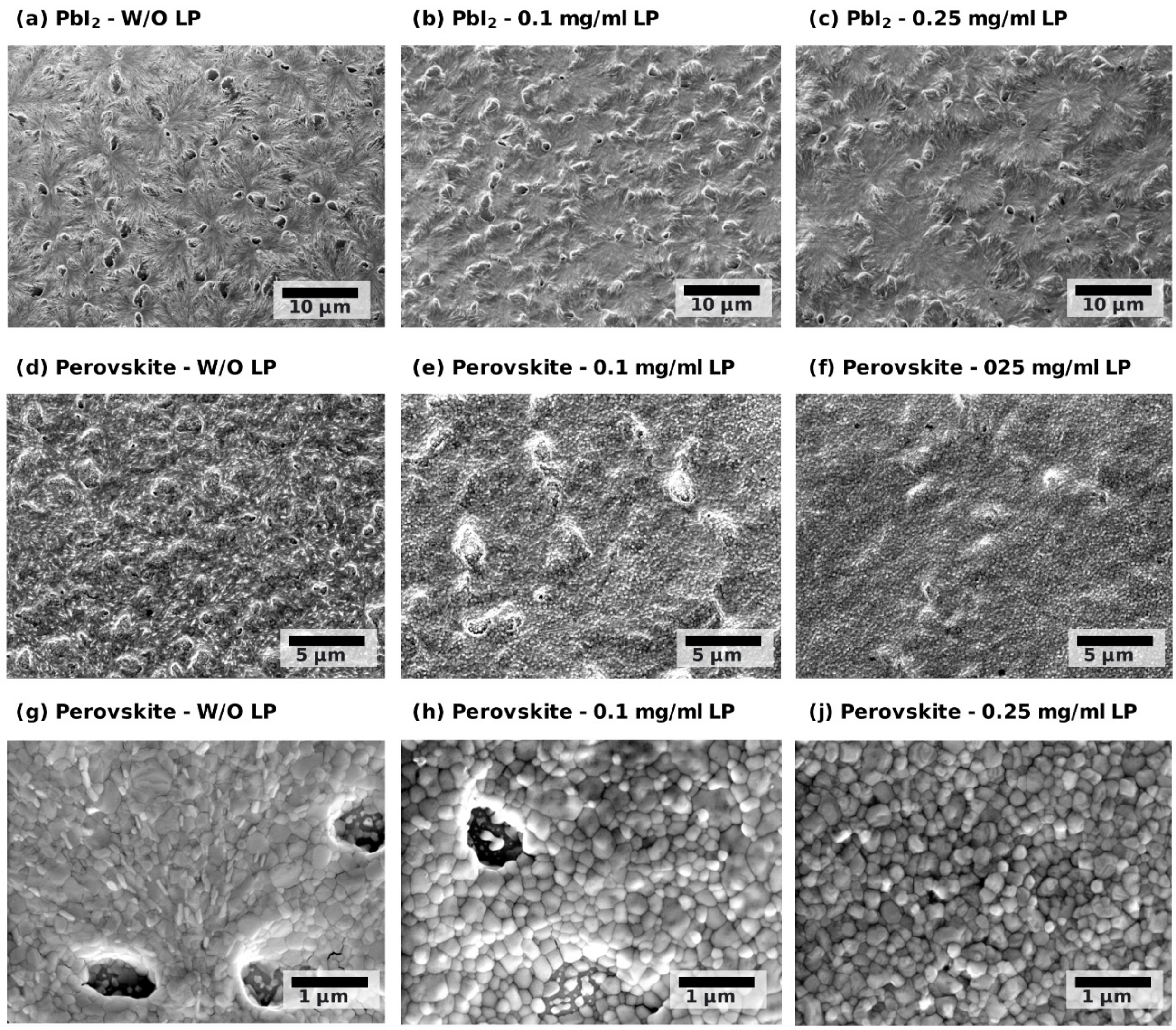

Figure S4. SEM images of blade-coated PbI_2-$(FAI)_{0.3}$-$(CsI)_{0.15}$ (a-c) and their corresponding double cation perovskite layer (d-f) deposited with incomplete drying condition without LP additive, with 0.1 mg/ml LP, and with 0.25 mg/ml LP respectively.

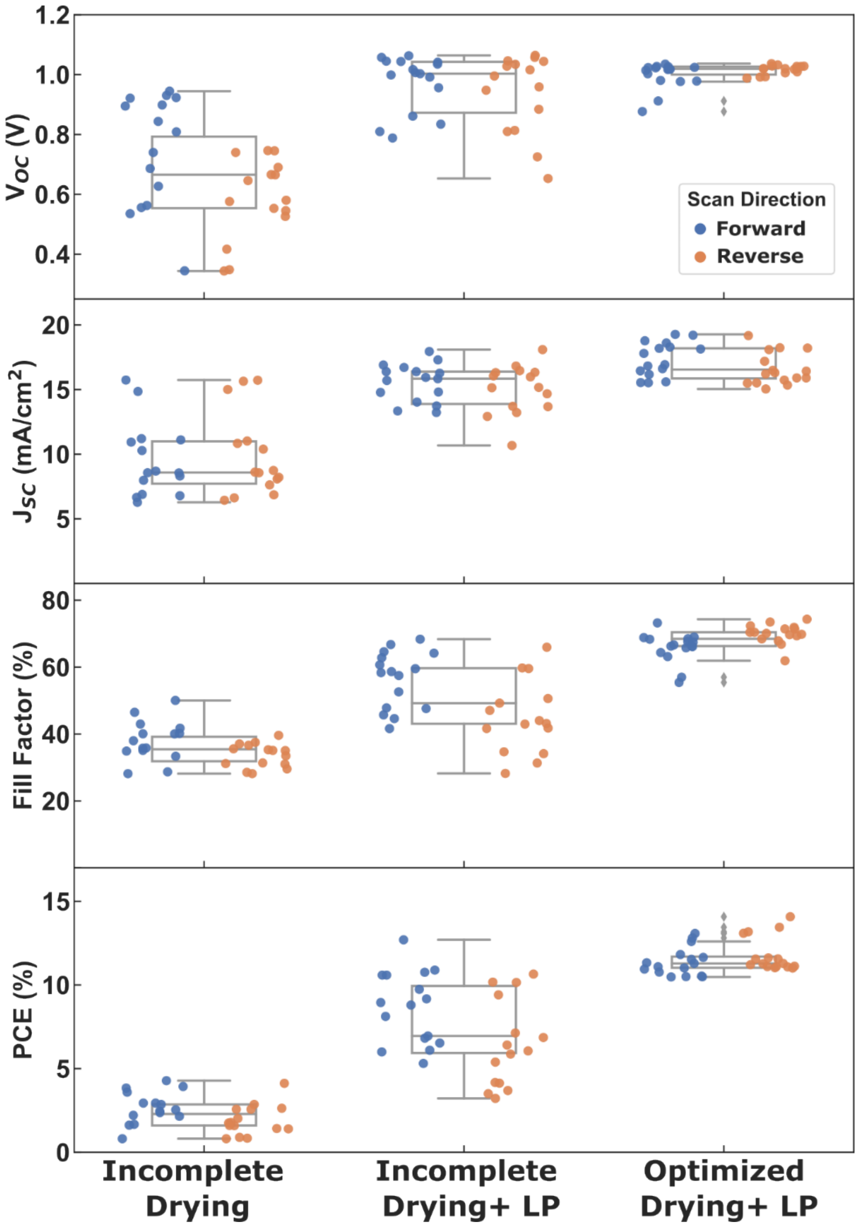

Figure S5- PV parameters of blade-coated flexible perovskite solar cells containing 16 cells obtained from one 5 × 7 cm^2 substrate in three conditions: incomplete drying, incomplete drying + LP, and optimized dying + LP.

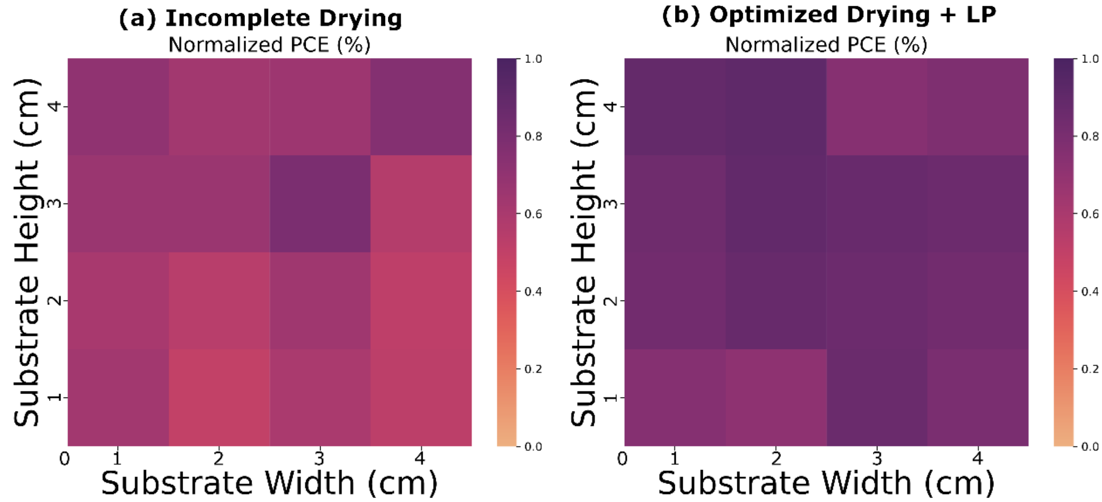

Figure S6- The mean normalized distribution of PCE across blade-coated substrates for incomplete and optimized drying.

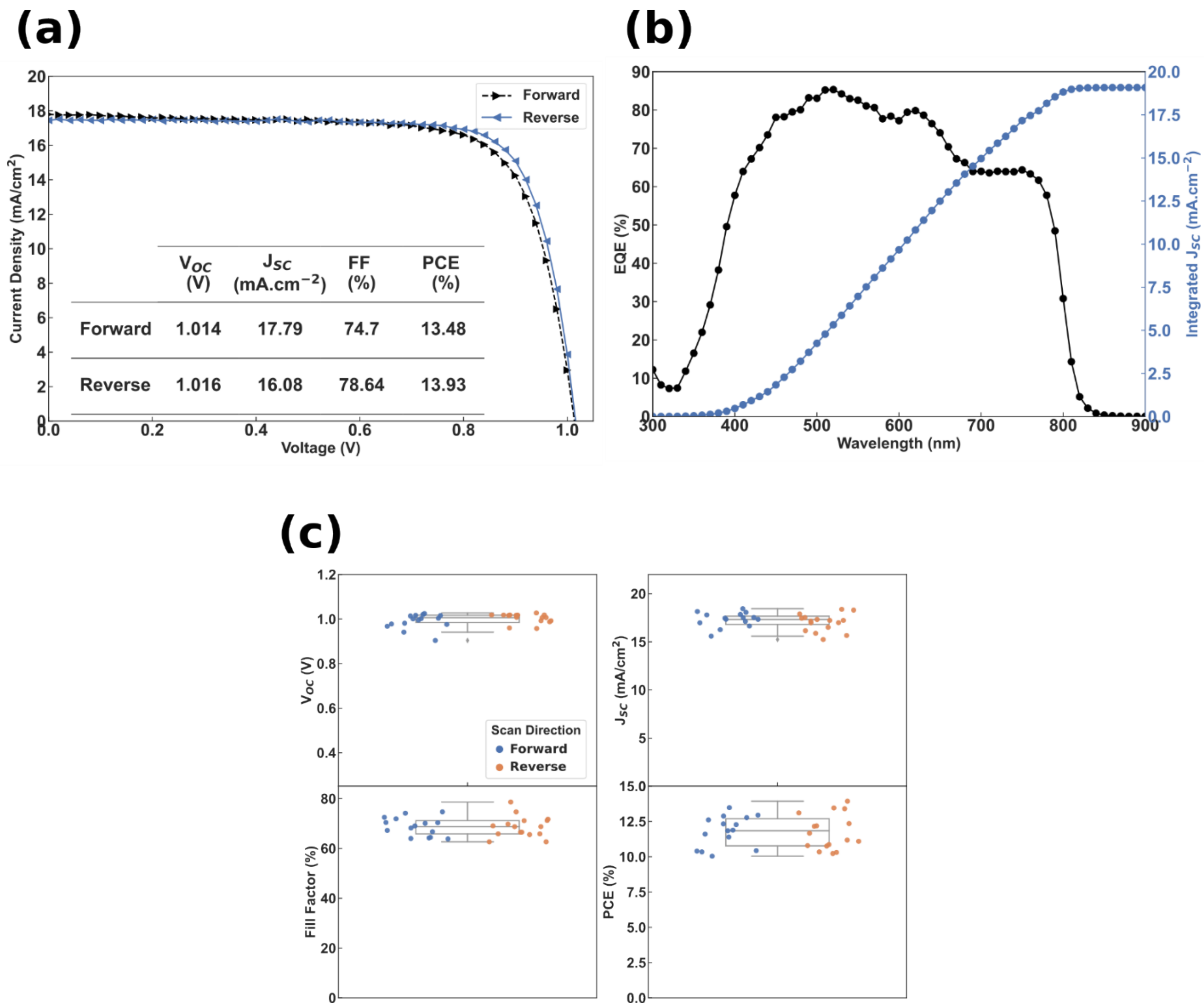

Figure S7- (a-b) JV Curve and external quantum efficiency of the champion all-bladed cell. (c) The box plots of PV parameters for all-bladed perovskite solar cells.

References

Castriotta, L. A., Fuentes Pineda, R., Babu, V., Spinelli, P., Taheri, B., Matteocci, F., Brunetti, F., Wojciechowski, K., & Di Carlo, A. (2021). Light-Stable Methylammonium-Free Inverted Flexible Perovskite Solar Modules on PET Exceeding 10.5% on a 15.7 cm2 Active Area. *ACS Applied Materials & Interfaces*. https://doi.org/10.1021/acsami.1c05506

Huang, Z., Hu, X., Xing, Z., Meng, X., Duan, X., Long, J., Hu, T., Tan, L., & Chen, Y. (2020). Stabilized and Operational PbI_2 Precursor Ink for Large-Scale Perovskite Solar Cells via Two-Step Blade-Coating. *The Journal of Physical Chemistry C*, *124*(15), 8129–8139. https://doi.org/10.1021/acs.jpcc.0c00908

Martin, B., Yang, M., Bramante, R. C., Amerling, E., Gupta, G., van Hest, M. F. A. M., & Druffel, T. (2020). Fabrication of flexible perovskite solar cells via rapid thermal annealing. *Materials Letters*, *276*, 128215. https://doi.org/10.1016/j.matlet.2020.128215